ASM Handbook, Volume 4F, *Quenchants and Quenching Technology*
G.E. Totten, R.S. Otero, X. Luo, L.C.F. Canale, editors
https://doi.org/10.31399/asm.hb.v4F.a0007010

Intensive Quenching Processes

Nikolai I. Kobasko, Michael A. Aronov and Joseph A. Powell, IQ Technologies, Inc.

INTENSIVE QUENCHING (IQ) is an alternative method of hardening steel parts. It provides extremely high cooling rates within the temperature range for martensite phase formation. This is in contrast to conventional quenching conducted in oil, polymer, or water, which limits the cooling rate within the martensite formation range. This rule is based on the belief that slower cooling will avoid a high tensile residual stress, distortion, and the possibility of the part cracking. However, extensive research conducted by Dr. Kobasko in the early 1960s in the Ukraine demonstrated that avoiding a high cooling rate when material is in the martensite phase is not always necessary or optimal for obtaining the best material properties. His studies showed that a very high cooling rate within the martensite range can actually prevent quench cracking, if performed correctly.

This phenomenon was discovered first by laboratory experiments (Ref 1). Figure 1 shows experimental data obtained for a cylindrical specimen made of low alloy steel with a diameter of 6 mm (0.24 in.). The bell-shaped curve clearly illustrates the general effect of the cooling rate within the martensitic phase on crack formation; the probability of quench cracking is low for both the relatively slow conventional quenching and also for rapid and uniform cooling (associated with the IQ process). Later, the IQ phenomenon was supported by the results of computer simulations and a large number of field experiments on a variety of actual steel parts.

Figure 2 shows a general correlation between the mechanical properties of steel parts and the cooling rates for both the conventional quenching process and the IQ process. Material mechanical properties improve with an increase of the cooling rate during quenching, because a faster rate of cooling results in a deeper hardened layer and a more complete phase transformation taking place in steel parts. A higher cooling rate produces a more complete phase transformations, finer part grains for a given alloy, and higher compressive surface stresses in the martensite surface during the quenching process (current compressive stress).

Currently, two types of IQ methods are used in heat treating practice: IQ-2 and IQ-3. IQ-2 is implemented in IQ water tanks, usually used for batch quenching of steel parts. IQ-3 is conducted in single-part processing, using high-velocity water flow IQ units. A detailed description of IQ technology, related equipment, and IQ applications are presented in detail in the book *Intensive Quenching Systems: Engineering and Design* (Ref 2). The sections below present an overview of IQ-2 and IQ-3 methods and equipment.

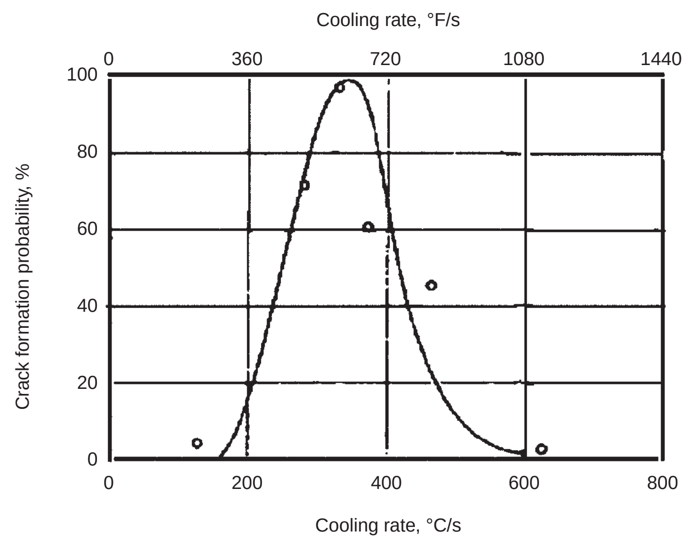

Fig. 1 Effect of cooling rate within martensite range on cracking of cylindrical samples of 6 mm (0.24 in.) diameter made of 40Kh steel (0.42% C, 0.60% Mn, 0.28% Si, 0.95% Cr, 0.25% Ni). Source: Ref 1, 2

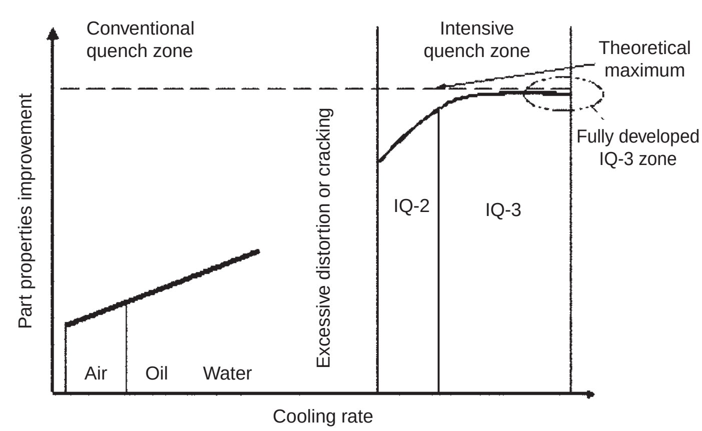

Fig. 2 General correlation between the improvement of mechanical properties of steel and cooling rate during quenching. Source: Ref 2

Batch Intensive Quenching Process

The batch IQ-2 process is a two- or three-step quench method. During the first step, parts are quenched in an IQ water tank for a specific period of time. The parts are then removed from the quench, and they continue cooling slowly in the air. If a deeper hardened layer or more complete phase transformation in the core is required, the part is put back into the IQ tank to complete quenching.

Specifics of Heat Transfer During Batch Intensive Quenching (IQ-2)

For a better understanding of the fundamentals of IQ methods, it is helpful to review the modes of heat transfer during the quenching of steel parts in liquid media. When parts are being quenched in oil, polymer, or water, four consecutive modes of heat transfer take place: shock nucleate boiling, film boiling, nucleate boiling, and convection (Ref 2). The heat flux from the part surface is high at the beginning of the quench, resulting in almost instant initiation of the shock nucleate boiling process. Due to the high heat flux during this mode of heat transfer, the rate of bubble formation is so great that, in a very short time period (usually approximately 0.1 seconds after the beginning of the quench), the bubbles merge with each other, forming a vapor blanket or film on the part surface. The heat flux from the part surface that is required for the initiation of the film boiling mode of heat transfer is the first critical heat flux density, $q_{cr}1$. Note that the formation of the vapor blanket is a very unstable process and therefore uncontrollable.

Prior to forming a full vapor blanket surrounding the entire part surface, areas of the film boiling move sporadically along the part surface, causing non-uniform cooling. In addition, the low thermal conductivity of the vapor blanket creates a thermal barrier for heat transfer from the hot surface of the part to the quenchant, resulting in a sharp reduction of the heat flux from the part surface and a slowing down of the cooling rate (Ref 2), similar to a gas quench. This non-uniform and delayed cooling under film boiling conditions may, in turn, cause an excessive and unpredictable part distortion and a spotty surface hardness, often called a slack quench.

Due to a gradual decrease of the cooling rate during film boiling, the temperature gradient throughout the cross section of the part likewise decreases, resulting in a reduction of the heat flux from the part surface. At some point, the heat flux on the surface of the part reaches a level at which it cannot support the film boiling process any longer. The vapor blanket begins to collapse, and the film boiling mode of heat transfer is replaced by the nucleate boiling mode (Ref 2–4). The heat flux at the part surface when the nucleate boiling process starts is the second critical heat flux density, $q_{cr}2$ (Ref 2). Due to the absence of the vapor blanket (a thermal barrier) on the part surface during the nucleate boiling phase, the heat flux from the part surface starts rising from $q_{cr}2$ to its maximum value. Note that the evaporative cooling in the nucleate boiling process is both a stable and intensive mode of heat transfer. The average heat-transfer coefficient (HTC) from the part surface during the nucleate boiling process is greater than that during the non-uniform film boiling process. In the final stage of conventional quenching, the nucleate boiling process is replaced by convection heat transfer from the part surface to the liquid quenchant, and the heat flux from the part surface further decreases.

In contrast to conventional quenching, IQ-2 eliminates the film boiling process due to vigorous quenchant agitation and special additives (salts) in small concentrations in the water. The nucleate boiling process initiates from the very beginning of the IQ-2 quench. The part surface temperature drops quickly to the temperature just above the quenchant boiling point and maintains this level until the nucleate boiling stops and a convective mode of heat transfer begins. The process of heat exchange between the part and the quenchant during the period of time when the part surface temperature stabilizes just above the quenchant boiling temperature is a self-regulated thermal process. This phenomenon was investigated by French in 1928, who measured the surface temperature of small and large spherical steel samples during quenching (Ref 5). French was the first to publish data showing that film boiling is completely absent and the surface temperature of the samples drops from 875 to 150 °C (1600 to 300 °F) in less than 0.82 seconds (Table 1). Further, the surface temperature remains at the level of the boiling point of the quenchant liquid (Fig. 3).

In 1928 there was no technology to correctly measure the overheating of the boundary layer in order to analyze the transient nucleate boiling process. That is why temperature measurements were taken in the interval of 875 to 150 °C (1600 to 300 °F). It was observed that film boiling was absent when steel samples were quenched in cold water. However, film boiling took place when spherical samples made of copper were quenched. Film boiling takes place on copper due to the high thermal conductivity of copper, which provides a high heat flux density exceeding the value of $q_{cr}1$. The thermal conductivity of steel is almost 20 times lower than that of copper. This lower thermal conductivity of steel provides a lower initial heat flux density, which is below the value of $q_{cr}1$, resulting in the elimination of the film boiling process. It was observed by French that the surface temperature drops almost instantly (within 1 second) to 150 °C (300 °F). Using accurate experimental data, the real HTCs were evaluated (Fig. 4). During the nucleate boiling process, HTCs are as high as those during the convection cooling process.

Table 1 Surface temperature versus time for steel spheres of different diameters when quenching from 875 °C (1600 °F) in 5% NaOH water solution at 20 °C (68 °F) moving with 0.9 m/s. Source: Ref 5

Diameter, mm	700 °C	600 °C	400 °C	300 °C	150 °C
6.35	0.027	0.037	0.051	0.09	0.69
12.7	0.028	0.042	0.071	0.11	0.60
25.4	0.033	0.042	0.074	0.13	0.82
63.5	0.023	0.039	0.093	0.14	0.59

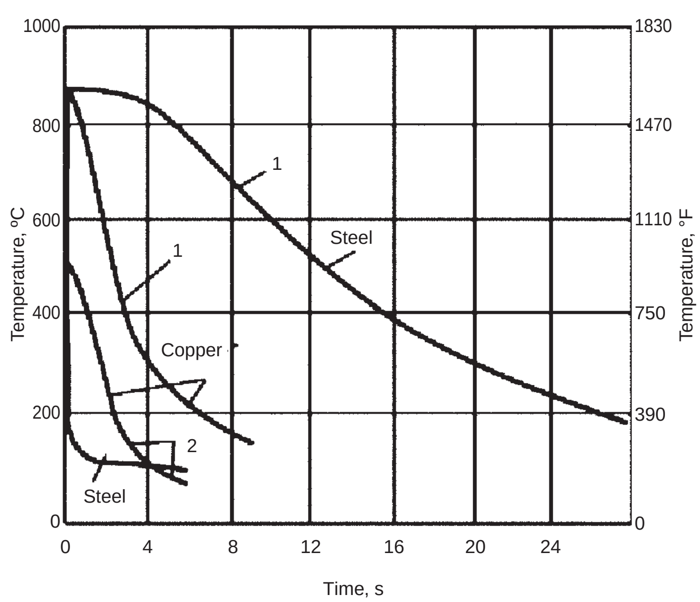

Fig. 3 Temperature at part surface and core versus time for steel and copper balls of 38.1 mm (1.5 in.) in diameter, quenched from 875 °C (1600 °F) in water at room temperature by French. 1, core; 2, surface. Source: Ref 5

As discussed in Ref 6, the classical law of Fourier should be modified to provide a finite value of heat distribution. The modified Fourier law is written as:

$$q = -\lambda \nabla T - \tau_r \frac{\partial T}{\partial \tau} \qquad \text{(Eq 1)}$$

The modified law of Fourier generates the hyperbolic heat conductivity equation, which provides a finite value for heat distribution (Ref 6).

Based on the experimental data of French and analytical solutions of the hyperbolic heat conductivity equation, one can conclude that the film boiling process can be completely absent when quenching steel parts in a cold liquid media because:

- A 5% NaOH water solution at 20 °C (68 °F) has a critical heat flux density, $q_{cr}1$, that is two times greater than that of cold water.
- Heat distribution rate is a finite value that cannot provide a high heat flux density, which can be less than the critical heat flux for film boiling.
- Prior to boiling, the cold solution must be heated up to the boiling point, and during this time the part surface temperature drops almost instantly to the liquid boiling point.
- Agitation increases the critical heat flux density, $q_{cr}1$, which in turn decreases the probability of the film boiling process initiation.

Taking into account the above facts, the authors of Ref 7 produced an analytical solution of the parabolic heat conductivity equation, with a non-linear boundary condition, for calculating the duration of the transient nucleate boiling process when film boiling is absent. As a result, simplified equations (Eq 2–4) were constructed for calculating the duration of the transient nucleate mode of heat transfer (self-regulated thermal process) (Ref 8–10):

$$\tau_{nb} = \left[0.24k + 3.21 \ln \frac{\vartheta_I}{\vartheta_{II}}\right] \frac{K}{a} \qquad \text{(Eq 2)}$$

$$\vartheta_I = \frac{1}{\beta}\left[\frac{2\lambda(\vartheta_0 - \vartheta_I)}{R}\right]^{0.3} \qquad \text{(Eq 3)}$$

$$\vartheta_{II} = \frac{1}{\beta}\left[\alpha_{conv}(\vartheta_{II} + \vartheta_{uh})\right]^{0.3} \qquad \text{(Eq 4)}$$

The thermal diffusivity values for stainless steel and Inconel-600 material and Kondratiev form coefficients which are presented in Table 2 and Table 3.

Generalized Equation for Calculating the Duration of the Self-Regulated Thermal Process

Using Eq 2, 3, and 4, a generalized equation for calculating the duration of the nucleate boiling process can be presented in the following simple form (Ref 9–11):

$$\tau_{nb} = \Omega k_F \frac{D^2}{a}. \qquad \text{(Eq 5)}$$

The value of Ω is a function of the convective Biot number. As an example, values for Ω and the Biot number are provided in Fig. 5 and Tables 4, 5, and 6 for the initial austenitizing temperature of 850 °C (1560 °F), bath temperature of 20 °C (68 °F), and different convective HTCs (776W/m^{2}K for still water and 4500 W/m^{2}K for highly agitated water). Note that when Bi approaches ∞, the value of Ω approaches 0. The real HTC changes drastically during the transient nucleate boiling process (Fig. 4) (Ref 2).

For developing optimal intensive quenching processes, special attention needs to be paid to the martensite start temperature (M_S) and finish temperature ($M_{F.}$). As seen from Fig. 6, if the Ms temperature is above the quenchant boiling temperature, the self-regulated thermal process delays martensite transformation during the transient nucleate boiling mode. If the quench is interrupted during this stage of cooling and the steel part is immediately tempered, martensite transformation will not take place; instead, a so-called austempering process in cold liquid will occur. This example shows that, when developing IQ processes, it is necessary to take into account M_S and M_F values.

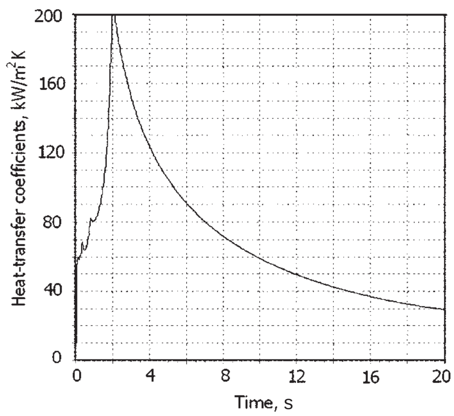

Fig. 4 Shock and nucleate boiling heat transfer coefficients versus time for a sphere of 38.1 mm (1.5 in.) in diameter quenched from 875 °C (1550 °F) in a 5% aqueous NaOH solution at 20 °C (68 °F). Source: Ref 2

Table 3 Kondratjev coefficient K, S/V, K(S/V) depending on different shapes and sizes of solid bodies. Source: Ref 2

Shape	Kondratjev coefficient K, m^2	$\frac{S}{V}$, m^{-1}	$K\frac{S}{V}$, m
Infinite plate of thickness L	$\frac{L^2}{\pi^2}$	$\frac{2}{L}$	$\frac{2L}{\pi^2}$
Infinite cylinder of radius R	$\frac{R^2}{5.784}$	$\frac{2}{R}$	0.346 R
Infinite square bar with sides of L	$\frac{L^2}{2\pi^2}$	$\frac{4}{L}$	$\frac{2L}{\pi^2}$
Cylinder of radius R and height Z	$\frac{1}{\frac{5.784}{R^2}+\frac{\pi^2}{Z^2}}$	$\left(\frac{2}{R}+\frac{2}{Z}\right)$	$\frac{2RZ\ (R+Z)}{5.784\ Z^2+\pi^2 R^2}$
Plate with sides L_1, L_2, L_3	$\frac{1}{\pi^2\left(\frac{1}{L_1^2}+\frac{1}{L_2^2}+\frac{1}{L_3^2}\right)}$	$\frac{2(L_1L_2+L_1L_3+L_2L_3)}{L_1L_2L_3}$	$\frac{2(L_1L_2+L_1L_3+L_2L_3)L_1L_2L_3}{\pi^2\left(L_1^2L_2^2+L_1^2L_3^2+L_2^2L_3^2\right)}$
Sphere	$\frac{R^2}{\pi^2}$	$\frac{3}{R}$	0.304R

Table 2 Thermal diffusivity and thermal conductivity of Inconel 600 and stainless steel depending on sample temperature (°C)

Temperature, °C	Inconel 600		Stainless steel AISI 304	
	$a \times 10^{-6}, m^2/s$	$\lambda, W/mK$	$a \times 10^{-6}, m^2/s$	$\lambda, W/mK$
100	3.7	14.2	4.55	17.5
200	4.1	16	4.63	18
250	4.3	9	4.66	18.8
300	4.5	17.8	4.7	19.6
400	4.8	19.7	4.95	21
500	5.1	21.7	5.34	23
600	5.4	23.7	5.65	24.8
700	5.6	25.9	5.83	26.3
800	5.8	26.3	6.19	27.8
900	6.0	28	6.55	29.3

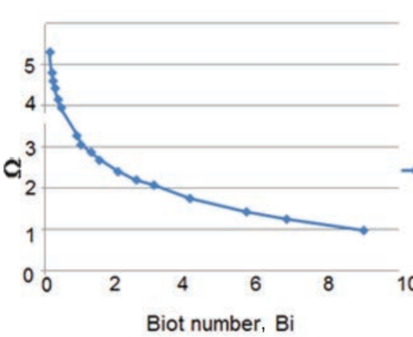

Fig. 5 Ω value versus Biot number (Bi) depending on size of steel part and HTC during convection. Adapted from Ref 12

Table 4 Duration of transient nucleate boiling process (τ_{nb}) for cylinders of different diameters when quenching in still water and convective HTC = 776 W/m^{2}K

Diameter, mm	Bi_{conv}	Ω	K·10^{-6}, m^2	τ_{nb}, sec
10	0.18	4.83	4.32	3.87
12.54	0.22	4.62	6.75	5.78
15	0.265.	4.44	9.8	?.8
20	0.353	4.18	17.2	13.3
25	0.441	3.96	27	19.8
50	0.882	3.30	108.1	66.1

Table 5 Duration of transient nucleate boiling process (τ_{nb}) for cylinders of different diameters (D) (when water flow is within 1.3–1.5 m/s and convective HTC = 4500 W/m²K)

Diameter, mm	Bi_{conv}	Ω	K, m²	τ_{nb}, sec
10	1	3.08	4.32×10^{-6}	2.5
12.5	1.28	2.88	6.75×10^{-6}	3.6
15	1.53	2.70	$9{,}8\times10^{-6}$	4.87
20	2.04	2.42	17.2×10^{-6}	7.71
25	2.56	2.21	27×10^{-6}	11.13
30	3.07	2.08	38.9×10^{-6}	15
40	4.09	1.76	69.17×10^{-6}	22.5
50	5.11	1.55	108.1×10^{-6}	34.9
80	8.18	1.102	276.7×10^{-6}	56.4

Table 6 Duration of transient nucleate boiling process (τ_{nb}) for austenitized steel when water flow velocity is within 1.3–1.5 m/s and convective HTC = 4500 W/m²K

Diameter, mm	Bi_{conv}	Ω	K, m²	τ_{nb}, sec
10	0.51	3.73	4.32×10^{-6}	1.5
12.5	0.64	3.50	6.75×10^{-6}	2.17
15	0.77	3.36	$9{,}8\times10^{-6}$	3.03
20	1.02	3.09	17.2×10^{-6}	4.88
25	1.28	2.87	27×10^{-6}	7.12
50	2.55	2.21	108.1×10^{-6}	22

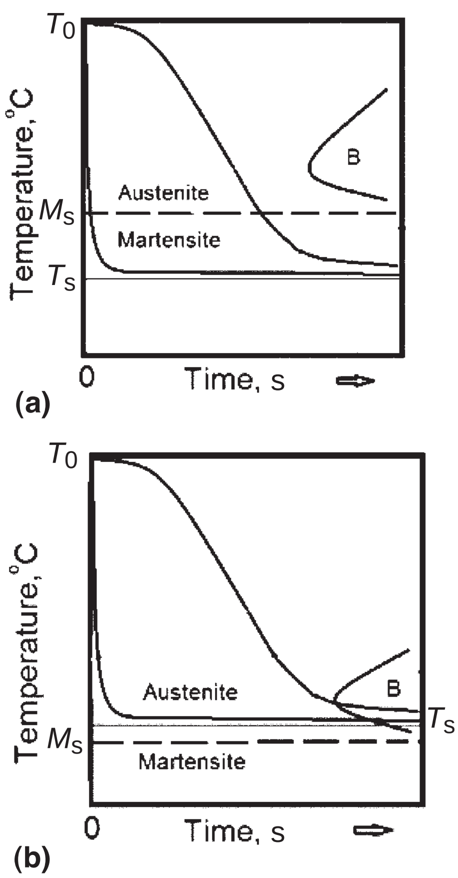

Fig. 6 Relationship between martensite start temperature (M_S) and self-regulated thermal process. T_S is saturation temperature, B is bainite

Table 7 provides these values, depending on the content of carbon in steel. High carbon steels should be quenched intensively to reduce the surface temperature of the part to the bath temperature within a short time, because the M_F temperature is below zero. If the IQ process is correctly designed, the service life of steel parts increases considerably due to the formation of more martensite with finer grains, as well as the presence of compressive residual stresses at the part surface.

Coupling of Transient Nucleate Boiling with Convective Heat Transfer

If the film boiling process is absent and transient nucleate boiling takes place immediately, the cooling process is governed by the equations (Ref 8, 9):

$$c\rho\frac{\partial T}{\partial \tau} = div(\lambda gradT) \quad \text{(Eq 6)}$$

$$\left[\frac{\partial T}{\partial r} + \frac{\beta^m}{\lambda}(T - T_S)^m\right]_{r=R} = 0 \quad \text{(Eq 7)}$$

$$T(r,0) = T_0 \quad \text{(Eq 8)}$$

After the transient boiling process is completed, a convection mode of heat transfer begins, and the third kind of boundary condition (Eq 9) is used instead of the boundary condition shown in (Eq 7):

$$\left[\frac{\partial T}{\partial r} + \frac{\alpha_{conv}}{\lambda}(T - T_m)\right]_{r=R} = 0 \quad \text{(Eq 9)}$$

The initial temperature for the convection mode of heat transfer is the temperature distribution at the end of the transient nucleate boiling process:

$$T(r,0) = T(r,\tau_{conv}) \quad \text{(Eq 10)}$$

This means that $T(r,\tau_{nb}{}^{end}) = T(r,\tau_{conv}{}^{start})$ and it is chosen as an initial condition for the convection heat transfer mode.

A transition from the nucleate boiling process to the convective mode of heat transfer is determined by equalizing the heat fluxes at the end of boiling and at the beginning of convection:

$$q_{nb} \equiv q_{conv}. \quad \text{(Eq 11)}$$

Thus, one should use the temperature distribution at the end of the nucleate boiling process as the initial temperature for the convection mode of heat transfer (Ref 12). Only this approach can provide accurate calculation of data. However, this is rather complicated task and needs to be developed further.

Single-Part Processing Intensive Quenching Process

The single-part processing IQ-3 method is a two-step quenching technique. During the first step, the part is quenched in a chamber with a uniform annulus around the part for uniform flow of high-velocity water in the IQ unit for a specific amount of time. Usually, the IQ-3 quench is interrupted at a time when surface residual compressive stresses are at their maximum value, the hardened layer is at an optimal depth, and the part core has not yet cooled to the Ms temperature (for the given alloy being quenched). The part is then removed from the chamber, and it continues cooling in the air. During air cooling, martensite surface layers are also self-tempering from the heat from the core. The boiling process does not take place on the part surface during IQ-3, since the water is flowing so fast that it does not have a chance to reach its boiling temperature. A so-called direct convection cooling is the mode of heat transfer taking place during IQ-3. To determine the optimal dwell time for the IQ-3 process, it is necessary to calculate HTCs for the high-velocity water flow conditions on the part surface, for the given part geometry and thermal properties.

Note that direct convection can take place during batch quenching as well, if the steel part is thick enough. According to Ref 2, direct convection takes place when this criterion is satisfied (Eq 12, 13):

$$Bi = \frac{2(\vartheta_0 - \vartheta_I)}{\vartheta_I + \vartheta_{uh}} \quad \text{(Eq 12)}$$

$$\text{Here } \vartheta_I = 0.293\cdot\left[\frac{2\lambda(\vartheta_o - \vartheta_I)}{R}\right]^{0.3} \quad \text{(Eq 13)}$$

where $\vartheta_0 = T_0 - T_S$; T_0 is the initial austenitizing temperature; $\vartheta_I = T_I - T_S$, T_I is the nucleate boiling start temperature; T_S is the saturation temperature; $\vartheta_{uh} = T_S - T_m$; T_m is the bath temperature; λ is the thermal conductivity of steel in W/m·K; R is the radius in m; and Bi is a Biot number.

Calculation of HTCs for High-Velocity Water Flow Within Channels

Forced-convection heat transfer coefficients for water flow within a channel or annulus

Table 7 M_S and M_F temperature versus content of carbon steel

Carbon, %wt	0.2	0.4	0.6	0.8	1.00	1.20	1.4	1.6
M_S, °C	450	350	300	250	210	180	140	100
M_F, °C	380	110	Below 0	Below 0	−100	−105	−110	−115

around the part shell are determined from this equation of similarity (Ref 13):

$$\overline{N}u = 0.021\ \text{Re}^{0.8} \cdot \text{Pr}^{0.43}(\text{Pr}_m/\text{Pr}_{sf})^{0.25} \cdot \varepsilon_e \qquad \text{(Eq 14)}$$

where Nu is the Nusselt number; $\text{Re} = \frac{wd_{eq}}{\nu}$ is the Reynolds number; and $\text{Pr} = \frac{\nu}{a}$ is the Prandtl number.

The channel equivalent diameter d_{eq}, is calculated from:

$$d_{eq} = \frac{4S}{u} \qquad \text{(Eq 15)}$$

where S is the channel cross-section area; u is the full perimeter of the channel; Pr_m is the Prandtl number for the quenchant farthest from the part surface; and Pr_{sf} is the Prandtl number for the quenchant near the part surface.

For round channels, the equivalent diameter d_{eq} is equal to the geometrical diameter d. If $l/d > 50$, then $\varepsilon_e = 1$. At $l/d < 50$ the values of $\left(\frac{\text{Pr}_m}{\text{Pr}_{sf}}\right)^{0.25}$ and ε_e are taken from Table 8 and Table 9.

Calculation HTCs for Water Jet Cooling

Typical round nozzle arrangements used for jet cooling are presented in Fig. 7. Average HTCs for impingement jet cooling can be calculated with an accuracy of about 15% using this dimensionless correlation (Ref 14):

$$\overline{N}u = K_1 \cdot K_2 \cdot \text{Re}^{\frac{2}{3}} \cdot \text{Pr}^{0.42} \qquad \text{(Eq 16)}$$

where

$$K_1 = \left[1 + \left(\frac{H/D}{0.6}\sqrt{f}\right)^6\right]^{-0.05}; K_2 = \frac{\sqrt{f}(1 - 2.2\sqrt{f})}{1 + 0.2(H/D - 6)\sqrt{f}}; f = \frac{(\pi/4)D^2}{A_{square(hexagon)}}$$

where D is the nozzle diameter; H is a distance from the nozzle to the surface; A is the area of the square or hexagon (Fig. 7); and f is a relative nozzle area in terms of geometric dimensions of the nozzle and cooled surface arrangements (for example, this parameter is equal to $0.25 \cdot (D/r)^2$ for a single round nozzle).

The dimensionless numbers K_1 and K_2 depend on the nozzle geometry and arrangement. The Reynolds number (Re) depends on the outlet quenchant velocity and the number (Pr) characterizing physical properties of the quenchant. The above dimensionless correlation (Eq 14) was developed for these conditions:

$$2000 \leq \text{Re} \leq 100000;\ 0.004 \leq f \leq 0.04;\ 2 \leq \frac{H}{D} \leq 12$$

A typical arrangement for slot-type nozzles is presented in Fig. 8.

A dimensionless correlation for determining HTC for slot nozzles is (Ref 14):

$$\overline{N}u = \frac{2}{3} f_0^{\frac{3}{4}} \left(\frac{2\text{Re}}{f/f_0 + f_0/f}\right)^{\frac{2}{3}} \cdot \text{Pr}^{0.42} \qquad \text{(Eq 17)}$$

where $f_0 = [60 + 4(H/S - 2)^2]^{-0.5}$; and $S = 2B$, where B is the slot nozzle width.

Residual Stress Distribution and Distortion Evaluation

IQ processes provide greater current (during the quench process) and residual surface compressive stresses compared to conventional quenching in oil. To compare the dynamics of stress formation during IQ and conventional quenching, computer modeling of temperature, stress, and structural conditions were conducted for a cylindrical part made of AISI 1045 steel. The results of the computer simulations are shown in Fig. 9 and 10. For 1045 steel, martensite starts forming in the surface layer of the part when its temperature reaches 320 °C (610 °F). Due to the greater specific volume of the martensitic structure, the larger volume BCT grains expand, creating compressive stresses for both the IQ process and the conventional oil quenching process. However, there is a significant difference in the stress formation dynamics between these quenching techniques.

As seen in Fig. 9 and 10, extremely high heat extraction rates during the IQ process result in a much greater temperature gradient throughout the cross section of the part; the martensite shell forms over a thermally swollen core. When the martensite starts forming in the surface layer during IQ, the temperature difference between the surface and the core is approximately 500 °C (930 °F), while for conventional quenching it is less than 100 °C (212 °F). While the martensitic structure is forming in the surface layer, the core of the part is shrinking thermally. The increased thermal shrinking under the martensite shell results in the surface layer being pulled inward, which causes higher current surface compressive stresses. This effect is much more pronounced for the IQ process, which starts forming a martensite shell in less than 0.2 seconds, versus the oil quenching process, which requires 18 seconds to form martensite (and current compressive stresses) on the shell of the part. During this 18 seconds, the additional core cooling that takes place in the oil quench means that a shell is formed over a thermally shrunken core. This thermal shrinkage of the core is not able to enhance the surface compression as much as the IQ-3 quench.

Table 8 $\left(\frac{\text{Pr}_m}{\text{Pr}_{sf}}\right)^{0.25}$ **versus pressure and temperatures of water at the time of transition from nucleate boiling to a single-phase convection cooling phase**

Water temperature, °C	Pressure, MPa	$\left(\frac{\text{Pr}_m}{\text{Pr}_{sf}}\right)^{0.25}$	Average
20	0.10	1.42	1.54
	0.20	1.48	
	0.27	1.51	
	0.36	1.54	
	0.48	1.57	
	0.62	1.59	
	0.79	1.61	
	1	1.62	
40	0.10	1.23	1.36
	0.20	1.31	
	0.27	1.34	
	0.36	1.36	
	0.48	1.39	
	0.62	1.41	
	0.79	1.43	
	1	1.43	

Table 9 Values of parameter $\varepsilon_l = f\left(l/d, \text{Re}\right)$ for turbulent water flow

	l/d								
Re	1	2	5	10	15	20	30	40	50
$1 \cdot 10^4$	1.65	1.50	1.34	1.23	1.17	1.13	1.07	1.03	1
$2 \cdot 10^4$	1.51	1.40	1.27	1.18	1.13	1.10	1.05	1.02	1
$5 \cdot 10^4$	1.34	1.27	1.18	1.13	1.10	1.08	1.04	1.02	1
$1 \cdot 10^5$	1.28	1.22	1.15	1.10	1.08	1.06	1.03	1.02	1
$1 \cdot 10^6$	1.14	1.11	1.08	1.05	1.04	1.03	1.02	1.01	1

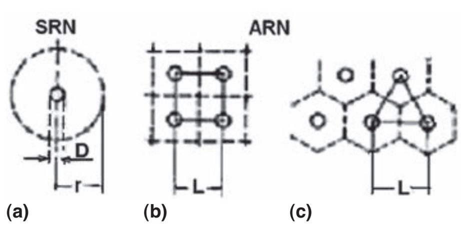

Fig. 7 Typical arrangement of nozzles. Adapted from Ref 2

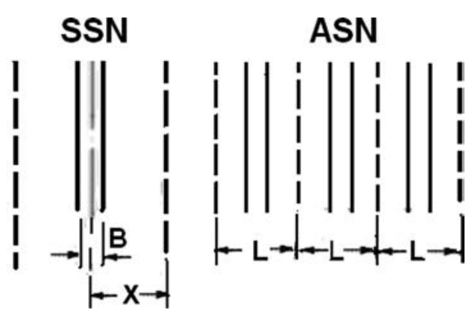

Fig. 8 Arrangement of slot nozzles in sprayer

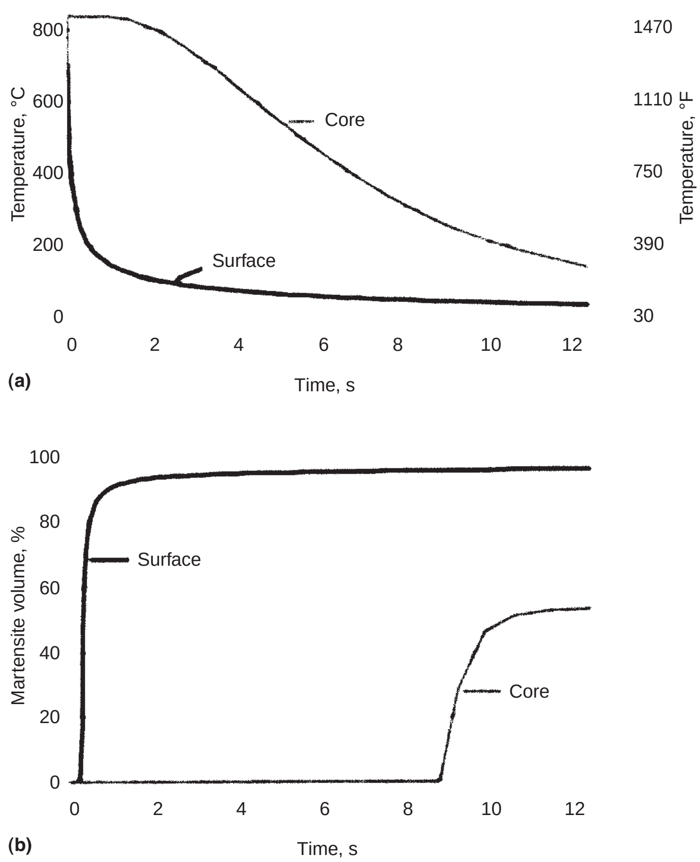

Fig. 9 Temperature and structural conditions during intensive quenching of a 25 mm (1 in.) diameter rod made of 1045 steel. Adapted from Ref 12

In addition, the IQ process provides a much deeper martensitic layer, resulting in a greater depth of the surface compressive stresses compared to that provided by the conventional oil quenching process. The subsequent formation of martensite in the core during intensive quenching ultimately results in the core swelling and a diminishing of the surface hoop compressive stresses. If core swelling is controlled by using a limited or lower hardenability steel (water-hardening grade) or interrupting the intensive quench before the core cools to the Ms temperature, the current compressive surface stresses can be maintained. However, as seen in Fig. 11, after IQ on 1045 material, the residual surface hoop stresses are still compressive and much greater than after oil quenching. The value of the residual hoop surface compressive stresses after the IQ process is 1000 MPa (–144.7ksi), while this value after oil quenching is −294 MPa (–42.5ksi). This is in spite of the fact that the core of the part is martensitic (and therefore stronger) after IQ, while it has a mixed structure after oil quenching.

The phenomenon of developing high residual surface compressive stresses after IQ for through-hardened parts made of higher hardenability steels (oil-hardening or even air-hardening grades of steel) is supported by considerable experimental data. Along with the uniformly fast cooling of the part shell, the key element of the IQ process is the interruption of the IQ at the proper time. The optimal cooling time depends on the shape and dimensions of the part, the type of steel, and ultimately the desired physical properties in accordance with the part specifications. For example, for parts made of through-hardened medium- and high-alloy steels, the quench is usually interrupted at the moment when surface compressive stresses are at their maximum value and the hardened layer of the part is at its optimum depth. A method for calculating the optimum dwell time during IQ was previously provided. After interruption of the intensive water quench, cooling continues in air. The thermal energy coming from the very hot part core tempers the martensitic surface layer, making it tougher and preventing possible cracking. On the other hand, for parts made of low- or medium-carbon steels with low hardenability, or for parts made of carburized grades of steel, the interruption criterion is often calculated to provide a hardened shell or case as deep as possible.

A common question regarding the IQ process is how it differs from induction case hardening (or shell hardening) methods. Like the IQ process, induction case hardening results in a part with high residual compressive surface stresses and with a wear-resistant martensitic surface. However, unlike the IQ processes, induction case hardening strengthens only the surface layer and does not toughen the core, since the core does not experience any martensite phase transformations. If core conditioning is required, the part must be through-heated to the austenitizing temperature, then quenched and tempered prior to conducting induction case hardening. This is in contrast to the IQ methods, which can provide high compressive surface stresses and, at the same time, strengthen (toughen) the core.

Additionally, induction case hardening creates hardness and residual-stress profiles that are much steeper in transition (from compressive at the surface to tensile below the surface) than those after IQ, because only a relatively thin surface layer of the part is austenitized by induction heating followed by quenching. Finally, the IQ process is interrupted when residual surface compressive stresses are at their maximum value, providing the part with an optimum hardened depth. The smoother hardness profile from surface to core, the high residual compressive surface stresses, the properly toughened core, and the optimum depth of hardness after IQ processes result in better part performance characteristics, all accomplished in a single process.

Due to the environmental benefits of IQ eliminating oil quenchants and using only water as the quenchant, the IQ process facilitates part-by-part heat treatment operations within the manufacturing cell. As mentioned earlier, high residual surface compressive stresses after the IQ process are due to a high-temperature gradient throughout the cross section of the part, at a time when martensite forms in the surface layer and establishes high current compressive stresses in the shell of the part. As an example, Fig. 12 presents experimental data on residual surface compressive stress profiles for cold work punches made of shock-resisting S5 steel (Ref 1). As seen from Fig. 12, residual surface stresses for the punch after quenching in oil are tensile at approximately 200 MPa (29 ksi), while these same stresses are compressive after IQ. The residual surface compressive stresses for the intensively quenched punch are in the range of approximately –500 to –950 MPa (–72 to –38 ksi). The surface stresses are still compressive at a depth of more than 0.5 mm (0.020 in.) from the punch surface. Note that the presence of residual surface compressive stresses changes the resistance of the IQ punches to wear—the punch becomes undersized, compared to the oil-quenched punches chipping; IQ-2 doubles the service life of the punch. This means the user obtains at least twice as many holes punched from IQ punches versus oil-quenched punches made of the same material and tempered to the same final hardness. Table 10 presents the improvement of S5 punch sample properties.

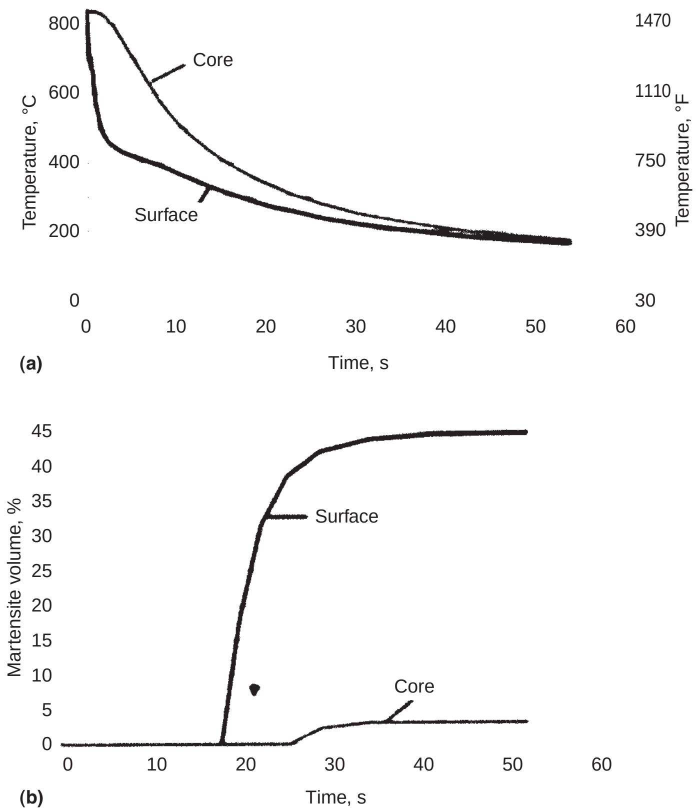

Fig. 10 Temperature and structural conditions during quenching in oil of a 25 mm (1 in.) diameter rod made of 1045 steel. Adapted from Ref 12

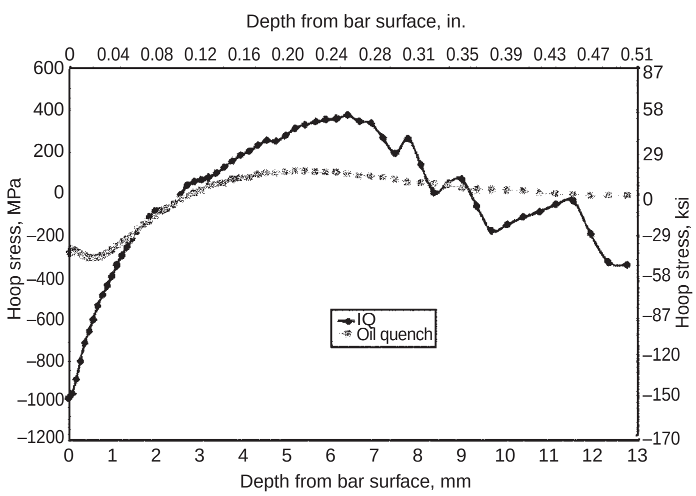

Fig. 11 Distribution of residual hoop stresses in 25mm (1 in.) diameter rod made of 1045 steel after intensive quenching and oil quenching. Adapted from Ref 12

An evaluation of intensive quenching processes has been conducted in Ref 2 and 21. A schematic of a high-velocity system for quenching cylindrical specimens is shown in Fig. 13. In this instance, the inner channel diameter of the quench system is 40 mm (1.6 in.) and the diameter of the specimen is 20 mm (0.8 in.). The water flow velocity in the channel is up to 19 m/s. Prior to the calculation of residual stresses, heat transfer coefficients in the working system were evaluated (Ref 15–18). The results of residual stress calculations and measurements are shown in Fig. 14. Through-hardened cylindrical specimens of 20 mm (0.8 in.) in diameter made of AISI 52100 steel were used for experimental evaluation of residual surface stresses. High-surface compressive residual stresses were obtained after intensive quenching for the above specimens (Ref 15–18). Note that the results of the calculations and experiments obtained by the authors of Ref 15 to 17 coincide directly with the conclusions reached by the authors of Ref 19 and 20.

Table 11 presents values for the surface residual compressive stresses for various actual parts and test samples. As seen from Fig. 14 and Table 11, very high surface compressive residual stresses are formed in through-hardened 52100 steel parts after intensive quenching. More uniform cooling during quenching results in less distortion of the part. However, in many cases, even with a uniform heat-extraction rate throughout the entire surface area, the part will distort due to its shape: thin sections of the part cool faster compared to thicker sections. This causes a non-uniform thermal contraction followed by a non-uniform formation of the martensitic shell with its phase change expansion. The dynamics of the IQ process usually reduce part distortion in such cases compared to conventional quenching in oil.

As an example, consider the distortion of a 25 by 250 mm (0.12 by 10 in.) keyway shaft with a 6.35 by 6.35 mm (0.25 by 0.25 in.) keyway made of AISI 1045 steel. Reference 2 presents the results of computer simulations of the distortion for the keyway shaft, as well as actual experimental keyway shaft distortion measurements after quenching in oil and after IQ in the IQ-2 water tank and in the single-part processing, high-velocity IQ-3 system. To simplify the evaluation of the keyway shaft distortion, one parameter characterizing the part deformation was used: shaft bow/flatness (Fig. 15).

The results of calculations show the following dynamics of keyway shaft distortion during IQ. At the very beginning of the quench (prior to the start of the martensite transformation on the part surface), the shaft is bowing toward the keyway due to the development of current tensile surface stresses in the thermally shrinking austenite at the keyway corners, which experience a greater thermal contraction compared to the rest of the shaft. Note that at the initiation of the quench, the hot shaft core is still at the austenitizing temperature and very low in strength. Therefore, the material in the shaft core is plastic and cannot resist the bowing of the shaft caused by thermal shrinking at the surface in the keyway corners. The direction of the bowing changes after the material at the keyway corners reaches the martensite start temperature. The formation of martensite causes the steel to expand, resulting in the development of current surface compressive stresses. These surface compressive stresses start to bend the shaft in the opposite direction (against the keyway). The reverse bending continues until the surface compressive stresses reach their maximum value. At this point, the thermally induced bow practically disappears. A continued phase transformation in

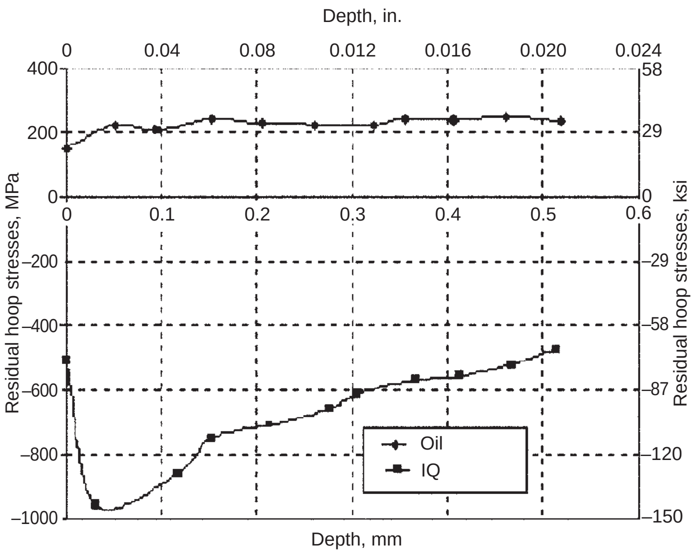

Fig. 12 Circumferential residual stresses for an S5 steel punch sample. Adapted from Ref 2

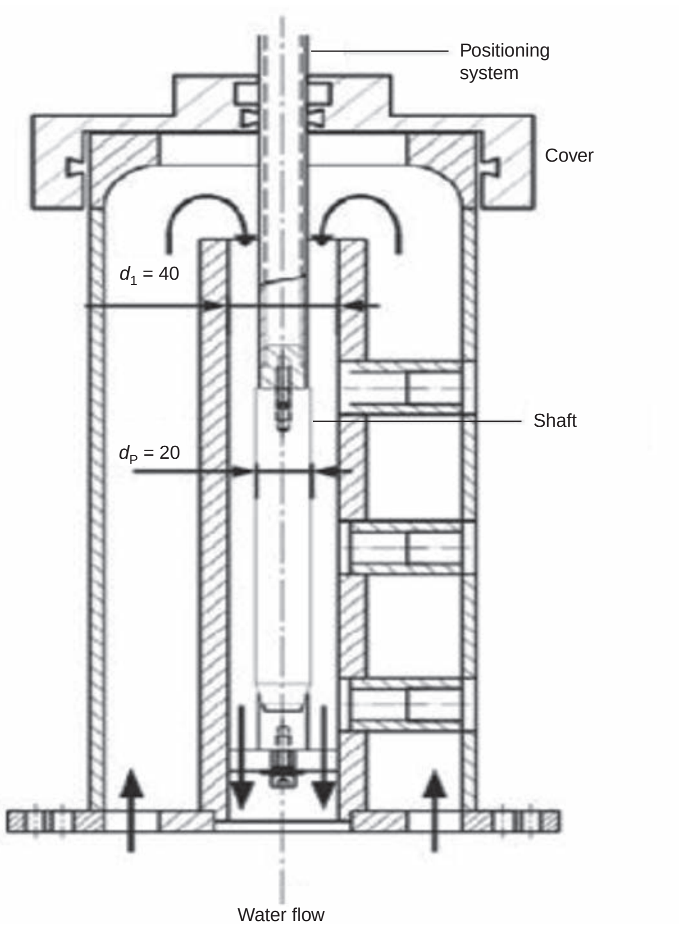

Fig. 13 Schematic of high velocity system for quenching cylindrical specimens installed at Bremen University in Germany. Adapted from Ref 15–18

the shaft causes swelling in the part core that partially cancels the compressive surface stresses. As a result, the shaft bows a little bit back toward the keyway.

A calculated value of the final shaft out of straightness after IQ is 0.098 mm (0.004 in.) (Ref 2). During conventional quenching in oil, the keyway shaft also bows first toward the keyway due to thermal shrinkage of the material prior to the start of the martensite transformation. Similar to IQ, the current surface compressive stresses created by material expansion start reversing the bowing of the shaft after martensite begins forming on the part surface in the keyway. However, because these compressive stresses are much lower compared to those formed during the IQ process, they cannot fully compensate for the thermally induced bow. After phase transformation is completed throughout the shaft, the core of the part swells, fully cancelling compressive stresses on the surface, causing a reversal of the bowing toward the keyway and increasing the final shaft distortion. Thus, at the end of oil quenching, in contrast to the IQ process, the keyway shaft is bent toward the keyway (Fig. 16). A calculated value of the final shaft out-of-straightness after quenching in oil is 0.871 mm (0.03 in.) (Ref 2). Table 12 presents experimental data (Ref 2) on the final distortion of the keyway shaft after the IQ processes and after conventional oil quenching.

Table 10 Improvement of S5 punch sample properties

Property		Oil quench	Intensive quenching
Hardness, HRC	As quenched	62–63	63–64
	After tempering	60–61	60–61
Impact strength, (N.m)	At 72 °F	1.36	4.8
	At 100 °F	3.4	6.12
Residual stress, (MPa)		200	−900

As seen in Table 12, both IQ methods provide much less final distortion than conventional quenching in oil. For symmetrical parts, the quench distortion can be as low as 50 microns. For example, the distortion for gear pump shafts made of carburized alloy steel and having a diameter of approximately 40 mm (1.6 in.) with a length of 385 mm (15.2 in.) was only 50 to 100 microns after quenching individually in the high-velocity IQ unit.

Note that intensively quenched parts will usually exhibit higher volumetric expansion and greater dimensions, compared to identical oil-quenched parts. For example, computer simulations (Ref 21, 22) conducted for a spur gear having 40 teeth, a module of 2.54, and a face width of 6.35 mm (0.25 in.) show that the intensively quenched gears expanded approximately 0.05 mm (0.002 in.) more in the radial direction compared to oil-quenched gears (0.18 versus 0.13 mm [0.007 versus 0.005 in.], respectively). The major reason for this is the differences in stress-state conditions during the faster martensite formation in the IQ process versus conventional oil quenching. In accordance with computer simulations and actual x-ray diffraction measurements, the magnitude of residual surface hoop stresses after IQ was approximately twice the value of hoop compression from oil quenching. While the parts after IQ may swell more, this distortion in part dimensional growth is predictable and repeatable, and can therefore be managed by adjusting the pre-heat treating (green) size of the part.

To develop a uniform, strong martensitic shell and residual surface compressive stresses, it is necessary to interrupt the IQ process after a certain dwell time, when the current residual surface compressive stresses are at their maximum value and their optimum depth. As the IQ processes provide repeatable distortion because of more uniform and intensive cooling, this creates high current compressive surface stresses that hold the part like a die. The full elimination of the non-predictable and non-uniform film boiling process means the green size of the part can be adjusted to provide a predictable quench-to-fit size change after quenching and tempering that needs less (if any) grinding, flattening, or straightening. Unlike random, non-uniform part distortion, a predictable part distortion becomes a so-called expected size change, which can be easily managed by the manufacturer. Therefore, the adjustment of green sizes can address the predictable dimensional changes resulting from the IQ process.

Improvement in Part Strength and Ductility

The IQ process often results in simultaneous improvement of both material strength and material ductility. This effect is sometimes referred to as material super-strengthening (Ref 23). The mechanism of additional strengthening of the material can be explained by the following points.

A residual super-cooled austenite in the surface layer of the part plastically distorts when it is subjected to high compression from the firm martensite plates that appear in the austenite. This results in the formation of a high density of dislocations in the hot austenite which provides finer grains of martensite. These finer grains improve the mechanical properties of the material after quenching and tempering. The higher the cooling rate within the martensite formation range, the greater the compression from the martensite plates, and the greater the density of dislocations in the contiguous grains. During rapid cooling, there is not enough time for dislocations to accumulate in the grain boundaries and to form nuclei for future micro cracks. The dislocations in the hot austenite freeze in the material. Thus, the rapidly forming martensite plates act like microscopic blacksmiths, forging the hot austenite under conditions of high current stress during intensive cooling as the expanding plates of martensite arise explosively, deforming the hot austenite and creating extremely high dislocation densities and finer martensitic grains.

Tables 13 and 14 show experimental data on the improvement in material mechanical properties resulting from IQ, compared to conventional oil quenching. Table 14 shows the improvement of the strength and plastic properties after accelerated cooling in the martensite formation range for different grades of steel (Ref 2, 12).

Summary of IQ Process Benefits

There are many benefits that derive from the IQ process, including:

- Higher surface hardness and core toughness with a greater hardened layer depth for parts made of carburized and non-carburized grades of steel
- Shortening of the carburization cycle for the same ECD (compared to oil quenching), resulting in the significant reduction of heat treatment processing costs and an increase of the production rate of the heat-treating equipment
- Improved part microstructure (finer grain and super-strengthened martensite)
- Greater and deeper residual surface compressive stresses
- Improved material strength (hardness), and at the same time toughness (ductility), a super-strengthening effect on the steel part
- Substitution of lower-alloy steels for reduced part costs, yet no penalty with regard to part strength or part performance
- Possibility of making high-power density parts—lighter parts with the same or better performance characteristics and fatigue life as oil-quenched parts due to the strengthening of the material and high residual surface compressive stresses provided by the IQ process
- Less part distortion and no part cracking with predictable size change that allows for a quench-to-fit net shape part after quenching and tempering
- Full elimination of quench oil and associated costs (cost of quench oil, part washing, etc.), resulting in a significant reduction of the heat treatment process cost and improved environment
- Possibility of moving heat treatment operations into the manufacturing cell for rapid, part-by-part heat treating, because the intensive water-quenching method is an environmentally friendly process

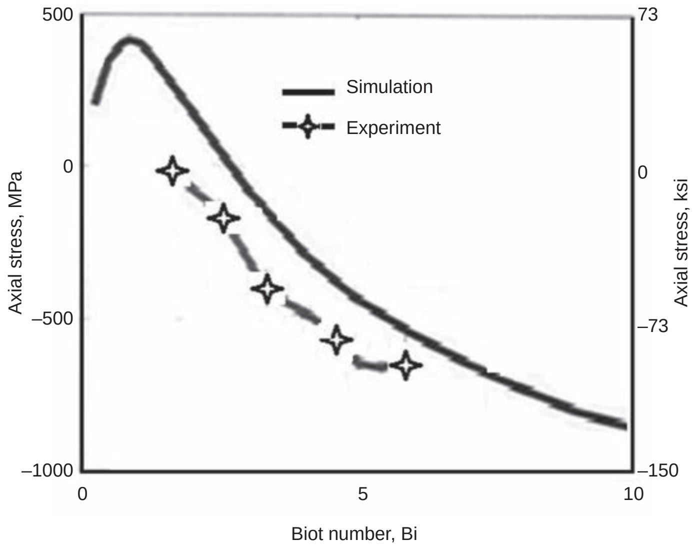

Fig. 14 Axial residual stresses versus Biot number received by computer simulation and experiments for AISI 52100 steel. Adapted from Ref 15–17

Table 11 Residual surface compressive stresses after intensive quenching and tempering. Source: Ref 12

Steel part	Residual hoop surface compressive stresses, MPa
52100 Roller Ø3″ (76 mm)	−840
52100 Roller Ø1.8″ (46 mm)	−900
4140 Kingpin Ø1.8″ (46 mm)	−563
S5 Punch Ø1.5″ (38 mm)	−750

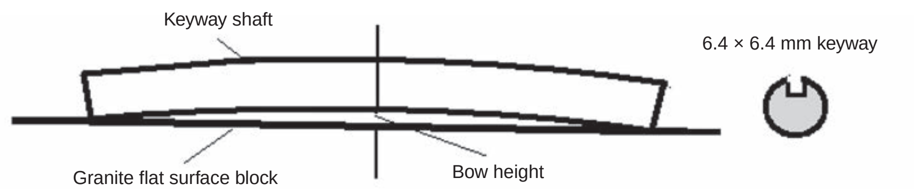

Fig. 15 Keyway shaft distortions. Adapted from Ref 2

Use of Optimal Hardenability Steels with a Uniform, Intensive Quench

For certain parts, the so-called optimal hardenability steel for a uniform and intensive quench is defined as a material that provides the part with maximum residual surface compressive stresses and an optimum hardened depth for maximum part strength and fatigue resistance. Kobasko reported in his studies (Ref 24–26) that traditionally used alloy steels may obtain optimal hardenability through application of the IQ processes. The optimal hardenability steel for a particular part should satisfy the fundamental correlation:

$$\frac{DI_a}{D} = 0.35 \pm 0.095 \qquad \text{(Eq 18)}$$

where

$$DI_a = f(DI, Form) \qquad \text{(Eq 19)}$$

Where DI = ideal critical diameter defined as a diameter of the round bar that has 50% martensite in its center, when the bar surface is cooled at an infinitely high rate (DI depends on the steel chemical composition); $Form$ = part form factor; DI_a= ideal critical size of a part of complex shape which is a copy of real steel part and has 50% martensite at its center when the small copy is cooled at an infinitely heat transfer coefficient; and D= part characteristic size (diameter for a cylindrical part, thickness for a plate, etc.).

According to Grossmann, the ideal critical diameter DI can be calculated as (Ref 3):

$$DI = 25.4 \times f_{Fe} \times f_{Mn} \times f_{Si} \times f_{Cr} \times f_{Ni} \times \ldots\ldots \qquad \text{(Eq 20)}$$

Values for hardenability factors f_{Fe} and f_x are provided in Ref 3 and 4.

A computer program was developed for determining the optimal steel chemical composition for a given part, with the aim of maximizing residual surface compressive stresses and part performance characteristics. The program uses Eq 18 and 20 and includes an algorithm for calculating the ideal critical thickness (DI_a) for parts of complex shapes based on critical diameter (DI) using Eq 19. For example, it was determined that intensively quenched AISI 1040 steel is optimal for truck semi-axles of 62 mm (2.4 in.) diameter. The chemical composition of 1040 steel is: 0.40C; 0.60 Mn; 0.30 Si; 0.10 Cr; 0.10 Ni; in wt. %. A calculated DI value of this steel using formula (Eq. 19) is:

$$DI = 25.4 \times 0.198 \times 3.00 \times 1.21 \times 1.216 \times 1.036 = 23\,.mm$$

For cylindrical parts $DI_a = DI$, therefore:

$$\frac{DI_a}{D} = \frac{23}{62} = 0.37 = 0.35 + 0.02$$

Table 15 presents fatigue test data for the axle made of standard 4340 steel quenched in oil and for recommended optimal hardenability 1040 steel intensively quenched. As seen from Table 15, fatigue resistance of the intensively quenched axle made of plain carbon 1040 steel was approximately 8 times greater than that of the oil-quenched axle made of higher alloy 4340 material. The use of 4340 steel for the intensively quenched axle would result in a more complete martensite transformation in the part core, causing much more core swelling compared to that for the 1040 steel axle, and cancellation of the residual surface compressive stresses, resulting in a shorter part fatigue life. Hence, while 4340 steel may be of optimal hardenability for the axle quenched in oil, it is not optimal for developing maximum surface compressive stresses in the axle when the part is intensively quenched.

In the early 1970s, Shepelyakovskii and colleagues suggested using steels of very low hardenability (LH) with the IQ process for relatively thin parts (such as bearings and gears) (Ref 27–30). Table 16 presents the chemical

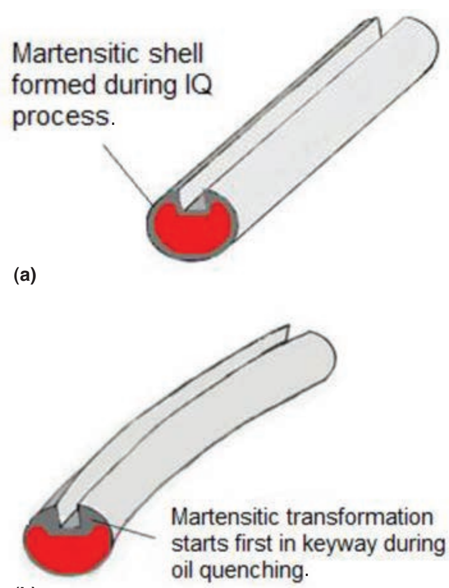

Fig. 16 Martensitic uniform shell formation in keyways during IQ process; (a) providing minimum distortion due to uniform shell formation during IQ process; (b) resulting in more distortion due to non-uniform shell formation during oil quenching (see Table 1). Adapted from Ref 2, 12

Table 12 Keyway shaft distortion experimental data (in mm). Source: Ref 2, 12

Single part oil quenching	Batch oil quenching	Single part intensive quenching
0.20 to 0.36	0.25 to 0.51	0.08 to 0.12

Table 13 Improvement in mechanical properties for plain carbon and alloy through-hardened steels. Source: Ref 23

Steel	Bar diameter, mm	Quench method	Hardness, HRC	Ultimate strength, MPa	Yield strength, MPa	Impact strength, J
1038	30	IQ	26	842	622	62
		Oil	23	807	532	28
1045	19	IQ	37	1191	1125	54
		Oil	32	980	766	53
	50	IQ	28	891	704	34
		Oil	27	880	626	31
1060	19	IQ	44	1485	1377	26
		Oil	40	1227	966	27
5160	19	IQ	48	1728	1584	22
		Oil	47	1592	1472	22
	38	IQ	48	1886	1499	9
		Oil	48	1623	1292	9
4140	19	IQ	48	1506	1181	40
		Oil	45	1350	1125	22
	50	IQ	44	1447	1072	20
		Oil	42	1329	1004	19

Table 14 Comparison of the mechanical properties of different steels quenched in oil and two-step quenched with accelerated cooling rate within the martensite range, when cooling in liquid nitrogen. Source: Ref 1, 2

Method	Cooling rate, °C/s	Steel	Ultimate strength, MPa	Yield strength, MPa	A (%)	Z (%)
Oil	3 – 6	U7A	1400	1250	4	–
		60C2A	1476	1355	8.5	–
IQ	30	U7A	1610	1570	7.9	31
		60C2A	1920	1740	5	22

Table 15 Fatigue test data for oil-quenched and intensively quenched truck semi-axles. Source: Ref 1

Quenching method	Steel grade	Numbers of cycles to fracture	Notes
Oil	AISI 4340	$(3.8–4.6) \times 10^5$	Semi-axles were destroyed
Intensive water spray cooling	AISI 1040	$(3.0–3.5) \times 10^6$	Test was suspended

composition of some of the LH steels recommended by Shepelyakovskii and Bezmenov (Ref 29). These steels are characterized by a low content of manganese, chromium, and other alloy elements. When through-heated and then quenched intensively, the LH steels produce a case-hardened layer and case microstructure with a properly toughened core that is similar to that of parts made of carburized grades of steel (Ref 30). These parts are subjected to a long carburizing cycle in a batch furnace. The use of IQ-3 and the optimal hardenability LH steels allows the use of single part flow and the elimination of long-cycle batch carburizing.

Table 16 Chemical composition of select low-hardenability steels. Source: Ref 29

Alloy	Steel 1	Steel 2	Steel 3	Steel 4	Steel 5	Steel 6
C	0.55–0.63	0.44–0.51	0.95–1.05	0.42–0.48	0.53–0.60	1.10–1.20
Si	0.10–0.30	0.10–0.25	0.15–0.30	0.40–0.65	0.40–0.80	0.15–0.30
Mn	<0.20	0.95–1.25	0.15–0.30	0.17–0.32	0.21–0.35	0.40–0.60
Cr	<0.15	<0.25	0.35–0.50	<0.25	<0.25	<0.25
Ni	<0.25	<0.25	<0.30	<0.20	<0.20	<0.20
Cu	<0.30	<0.30	<0.25	<0.15	<0.20	<0.20
Ti	0	0.06–0.12	0	0	0	0.06–0.12
S	<0.04	>0.04	<0.027	<0.04	<0.04	<0.04
P	<0.04	>0.04	<0.02	<0.035	<0.04	<0.04
Application	Gears	Semi-axles and shafts	Leaf-springs	Common Springs	Crank-shafts	Hard-working parts

Intensive Quenching Equipment

There are two general types of IQ equipment: IQ water tanks for implementing the IQ-2 process (either for batch operations or for continuous operations), and single-part processing high-velocity IQ-3 units. The three key elements of the IQ processes dictate the IQ equipment design regardless of its type:

- Intensive quenching uses highly agitated plain water or a low concentration of water and salt (mineral or organic) solution as a quenchant (no oils or polymers).
- For any type of the IQ process, it is necessary to provide a properly intensive, high heat-extraction rate uniformly over the entire surface area of the part from the beginning of the quench.
- It is necessary to interrupt the IQ process at the proper time to maximize compressive surface stresses.

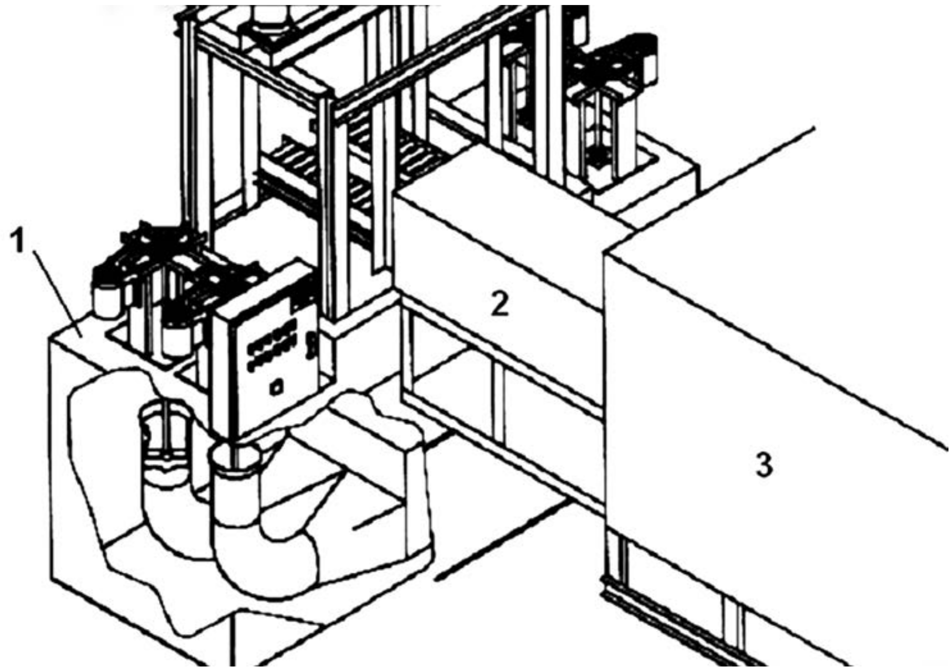

Fig. 17 Schematic of production stand-alone 6,000-gallon IQ system. 1-water quench tank equipped with propellers; 2-load charge car; 3-radiant tube

Batch-Type IQ Equipment

Designs for batch-type IQ equipment are similar to those for the equipment used for conventional oil quenching or batch polymer-water quenching. There are two types of batch IQ-2 equipment in operation: a standalone IQ-2 water tank installed at Akron Steel Treating Co. (Akron, Ohio, USA; it has been in production since 1999) and an IQ-2 water tank integrated in an atmosphere furnace installed at Euclid Heat Treating Co. (Cleveland, Ohio, USA; in production since 2003). Figure 17 presents a schematic of the production batch-type IQ-2 system equipped with a standalone IQ water tank. This system includes a radiant tube atmosphere box furnace with a work zone of 91 by 91 by 122 cm (36 by 36 by 48 in.), and a standalone IQ water tank of 22.7 m3 (6,000 gal.). A load transfer cart is used for moving the work from the furnace to the quench tank. The mild steel IQ tank is equipped with four propellers rotated by four motors for uniform and intensive flow of quenchant over the load of parts. The quenchant flow velocity in the tank is approximately 1.5m/s (5 ft/s) as it passes over the parts. A water–sodium nitrite solution of low concentration (8 to 10%) is used as a quenchant. An air-cooling system maintains the quenchant temperature below the required limit. The production IQ-2 system is designed for batch quenching loads of up to 1135 kg (2500 lb.).

Figure 18 shows a production integral quench atmosphere furnace of 91 by 91 by 182 cm (36 by 36 by 72 in.) equipped with an IQ water quench tank of 41.6 m^3 (11,000 gal.) (Ref 2, 12). The furnace is equipped with an intermediate controlled atmosphere chamber connecting the heating chamber to the IQ tank to ensure that water vapor from the quenchant does not contaminate the furnace atmosphere. The furnace atmosphere enters the intermediate chamber through two openings in the furnace door and leaves through the vent. The IQ-2 tank is equipped with four propellers rotated by four motors and with a loading/unloading quench elevator mechanism that provides a fast introduction of the load into the quench tank and removal of the load from the tank. The loading/unloading time is within about 2 or 3 seconds regardless of the load weight, which ensures a small difference in cooling times between the lower and upper layers of the load.

Fig. 18 Integral quench atmosphere furnace equipped with 41m^3 IQ water tank manufactured by AFC-Holcroft and installed at Euclid Heat Treating Co.

Similar to conventional quenching, a short shock-nucleate boiling process initiates at the very beginning of the IQ process in IQ-2 water tanks. However, in contrast to conventional quenching, the shock nucleate boiling process never transforms into the film boiling process.

Thus, only two modes of heat transfer take place during quenching in IQ water tanks: the transient nucleate boiling process followed by convection cooling. The film boiling process is fully eliminated due to the vigorous agitation of the quench bath through the load as well as the maintaining of the water temperature close to the ambient temperature and using a small amount of water additives (usually mineral or organic salts that affect the electrostatic conditions of the thin quenchant layer bearing against the part surface, resulting in an increase of quenchant surface tension and its resistance to film boiling). All of these factors increase the value of the first critical heat flux density ($q_{cr}1$) in the quench water. In other words, a greater heat flux from the surface of the part is required to bring the quenchant to the saturated temperature needed to initiate the film boiling process.

When parts are being quenched in batches in IQ water tanks, it is important to keep proper spacing between the parts. If a load is too dense, a local film boiling process can take place between the contiguous steel parts due to the reduced water flow velocity and the increased hydraulic resistance to the quenchant flow. One of the effective ways to minimize the possibility of initiation of the film boiling process during IQ-2 is the use of emitters in IQ water tanks (Ref 31, 32). Emitters provide water pulsations in the quench tank, resulting in a resonance effect with existing local films. The resonance effect destroys local films immediately after their initiation (Ref 32). Figure 19 presents some examples of production loads processed in IQ water tanks.

Fig. 19 Examples of production loads processed in IQ water tanks

Single-Part Processing IQ-3 Equipment

Single-part processing IQ-3 equipment is designed for quenching parts one at a time in the IQ unit quench chamber with a high-velocity water flow in the annulus between the quench chamber and the hot part, or by jet impingement on the hot part surface (Ref 33). The parts can be through-heated to the austenitizing temperature prior to quenching in a furnace or by induction through-heating. Figure 20 shows the layout of the typical single-part processing IQ-3 system. The IQ-3 quench sequence progresses in this manner: with the pump operating and the three-way valve in the bypass position, an austenitized part is placed in the lower section of the quench chamber. The air cylinders move the lower section up to the stationary upper section while locking and sealing the quench chamber in place. The three-way valve switches from the bypass to the quench position, and the water starts flowing through the quench chamber and over the austenitized part. When the IQ process is completed, the three-way valve switches back to the bypass position, and the water stops flowing through the quench chamber and again recirculates through the bypass line.

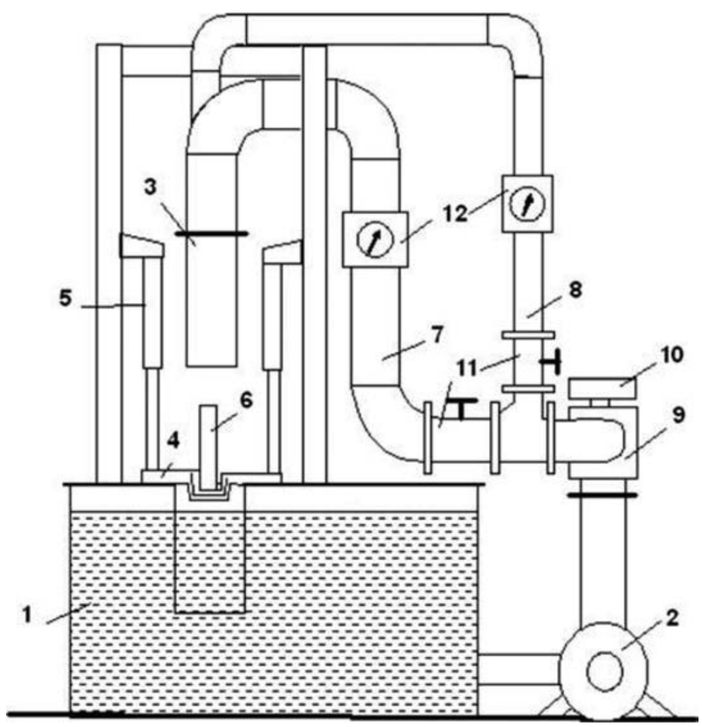

Fig. 20 Layout of typical single-part intensive quenching system. 1, water tank; 2, water pump; 3, stationary upper section of vertical quench chamber; 4, movable loading lower section of quench chamber; 5, air cylinders that move lower section up and down; 6, part to be quenched; 7-8, two of three water lines providing water flow through the quench chamber, and one bypass water line (not shown) used in idle conditions immediately before and after intensive quench dwell time of the part; 9, three-way valve providing water flow from the pump, either through the quench chamber or through the bypass line; 10, three-way valve actuator; 11, valves controlling water flow to quench chamber; 12, flow meters on water lines. Adapted from Ref 12

The air cylinders open the quench chamber by moving the lower section down. The part is removed from the lower section of the quench chamber, and the part finishes cooling in the air. In IQ-3 systems, control valves and flow meters, along with properly designed part-holding fixtures in the quench chamber, are used to adjust and control the water flow uniformly and intensively around all surfaces of the part. The major issue to address when designing single-part quenching IQ-3 systems is providing high-velocity water flow uniformly around the entire surface area from the initiation of the quench. This is an especially difficult task when processing parts of complex geometry (Fig. 21), which may cause the presence of stagnation zones at some areas of the part. The stagnation zones, in turn, may cause local film boiling, resulting in excessive distortion or even cracking.

Computational fluid dynamic modeling is often required for designing an optimum quench chamber configuration in the case of processing of complex-shaped parts (Ref 34). Figure 22 presents a picture of a high-velocity IQ system designed for processing gear products and shafts. The IQ system is capable of also quenching rings, rollers, and other parts with maximum dimensions of 200 by 500 mm (8 by 20 in.). The IQ-3 system is equipped with a chiller for maintaining proper water temperature and an atmosphere box furnace for austenitizing the parts. This system is installed at the IQ Center located at Euclid Heat Treating Co. Figure 23 shows an automated, single-part production IQ-3 system for processing shafts and gears equipped with an atmosphere rotary hearth furnace, pick-and-place device, and chiller.

IQ-3 provides the ultimate intensive cooling rate for steel parts during quenching which yields the highest as-quenched hardness and deepest quenched layer (versus conventional oil or polymer/water quenching). IQ-3 thus provides the maximum achievable improvement in grain refinement and in material mechanical properties for a given alloy of steel in a given geometry. Figure 24 shows some examples of steel parts quenched in single-part processing IQ-2 and IQ-3 units.

One of the major limitations for applying the IQ processes is the part dimensions and shape. The part thickness should be adequate for developing the required high temperature gradient throughout the part which is necessary for formation of the high current and high residual surface compressive stresses by controlling the swelling of the core. The minimum permissible part thickness depends on the shape of the part as well as on the type of steel; steels of low hardenability and carburized grades of steel allow for successful intensive quenching on thinner parts. Based on the results of numerous IQ process studies, the IQ method, in general, is not recommended for parts with a thickness of less than 10 mm (0.4 in.). The IQ process is not applicable to parts with a significant thickness variation, because it is practically impossible to assign a cooling time suitable for all sections of the part that will uniformly maximize surface compressive stresses while minimizing core swelling. (The thin sections of the part could be cooled completely prior to the quench interruption, resulting in excessive core swelling, part distortion, or even part cracking.)

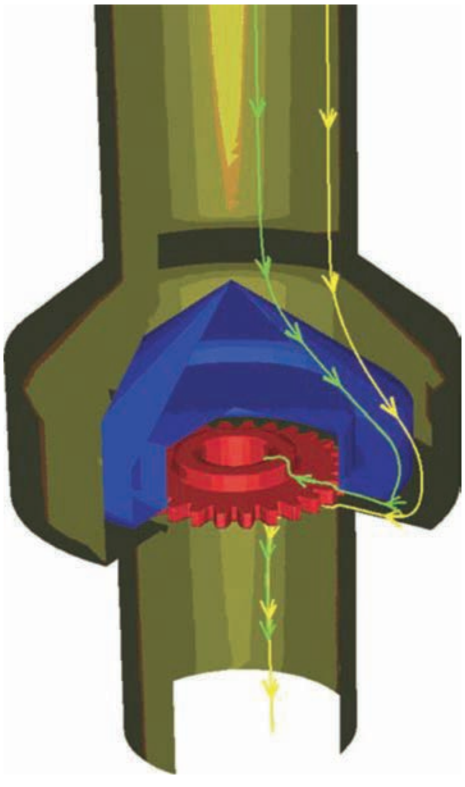

Fig. 21 Cutaway view of the quench fixture showing the gear (red), upstream reflector (blue), and representative water path lines passing over and under the gear (green, yellow). Adapted from Ref 34

Fig. 22 Single-part processing IQ system installation at the IQ Technologies Center at Euclid Heat Treating Co.

Intensive Quenching of Forgings Immediately After Hot Forging Operations

The first studies on the effect of quenching right after the completion of plastic deformations of steel parts (hot forging) were conducted in the former Soviet Union in the 1960s and later in Japan in the 1980s (Ref 35–38). It was demonstrated that quenching immediately after hot forging is completed improves material mechanical properties (tensile and yield strength, elongation, and reduction in area) by more than 20%, compared to quenching after conventional post-forging heat treatments (cooling of forgings in the air to room temperature, reheating for normalizing, and then reheating parts a third time for quenching and then tempering).

Fig. 23 Fully automated single-part processing IQ-3 system equipped with a controlled atmosphere rotary hearth furnace, pick-and-place device part transfer automation, and a water quenchant chiller

Fig. 24 Examples of parts quenched in single-part processing IQ units

Fig. 25 Portable 600-gallon DFIQ™ system for quenching hot forgings directly after the trim die

The studies also showed that the optimal temperature for thermomechanical treatment is 900 to 930 °C (1650 to 1705 °F) and the optimal deformation is 25 to 35%. The mechanical properties of the material improve due to the so-called freezing of more of the dislocations in the hot austenite steel grains created during the plastic deformation of the hot part. The mechanical properties of forging also improve due to the formation of finer grains (finer martensitic microstructure) in the material, compared to conventional plastic deformation processes when parts are cooled slowly in the air after forging and the dislocations are allowed to relax.

Combining the thermomechanical treatment with the IQ process is discussed in Ref 38. It was concluded that intensive quenching directly after forging may provide better mechanical properties as compared to using conventional post-forging heat treatments. Quenching immediately after forging was not commercialized for two major reasons: conventional quenching in oil is not suitable for forging shop operations because of the obvious fire hazards, and the use of conventional water or water polymer quenching is applicable only to forgings made of water-quench grades of steel or to parts of relatively simple shapes due to a high probability of crack formation. Use of the direct-from-forge intensive quenching (DFIQ™) process allows the manufacturer to overcome the two above hurdles for forging shops and to optimize the benefits of high temperature thermos-mechanical treatment (Ref 39) while using less energy to harden a forged part.

To test the DFIQ process, IQ Technologies Inc designed and manufactured a portable 600-gallon DFIQ system for quenching forgings immediately after plastic deformations are completed (this project was funded by the United States Department of Defense) (Fig. 25).

The major DFIQ system components include: steel tank; pump; special quenchant agitation system for providing the hot forging with the required uniform and intensive heat extraction rate required by the IQ process; conveyor to transport the part through the quenchant to allow it to finish cooling in the air; loading/unloading table; "sludge buster" for filtering the forging scale from the water quenchant; chiller for maintaining the quenchant temperature within an allowable range; and system controls. An environmentally friendly Daphne® "Genuine IntensiQuench®" quenchant is used in the DFIQ system. This quenchant is an optimal concentration solution of organic salts in plain water. IQ Technologies Inc jointly developed the quenchant with Idemitsu Kosan Co. of Japan.

The combination of the uniform and intensive delivery of the quenchant to the hot part surface in the DFIQ unit, combined with the unique cooling properties of the quenchant fluid, minimizes the duration of the initial film boiling stage of cooling (even from 1093 °C [2000 °F]). The dynamics of the uniform and intensive cooling of the hot forging surface shell result in a more uniform and complete grain transformation in the forging, and drastically reduce the probability of the part cracking.

A number of DFIQ trials were conducted in 2016 and 2017 with actual hot forgings in production conditions at three forge shops: Bula Forge and Machine of Cleveland, Ohio, USA; Welland Forge of Ontario, Canada; and Clifford Jacobs Forge of Champaign, Illinois, USA (Ref 39). Pictures of some the forgings processed in the DFIQ unit are presented in Fig. 26. The processed forgings were made of various steels (plain carbon, alloy, and high-alloy). The mechanical properties and microstructure obtained for the DFIQ forgings were compared to those of the same forgings processed using standard post-forging heat treatments. Table 17 presents data on mechanical properties obtained for the "key" forgings made of AISI 4140, 4340, and 8640 steels. The conventional heat treatment included cooling the keys in the air after forging (no separate normalizing process) followed by oil quenching and tempering. The DFIQ keys were tempered after quenching to provide the same hardness as the oil quenched and tempered keys. As seen from Table 17, the DFIQ process improved all material mechanical properties.

Table 18 presents the mechanical properties obtained for standard and DFIQ pintle adapters. Standard pintle adapters are made of 4340 steel. The standard heat treatment process for these parts is to allow them to cool in the air after forging, then anneal, normalize, quench, and temper. The pintle adapters were tempered only after DFIQ. As seen from Table 18, the DFIQ pintle adapters made of standard 4340 steel and of lower alloy 4140 steel both met the specs. The use of the DFIQ process allowed eliminating all post-forging heat treatment operations for these parts (except tempering), resulting in significant reduction of the heat treatment cost and production lead times.

An analysis of the results obtained showed that steel grain size after forging plays a crucial role in the effectiveness of the DFIQ process. It was demonstrated that the DFIQ process improves the mechanical properties only for forgings with an ASTM grain size of not less than 7.0. There was no improvement in mechanical properties for forgings with a grain size between 5.0 and 7.0. The mechanical properties of DFIQ forgings with a grain size below 5.0 were actually worse compared with those of standard forgings, although they

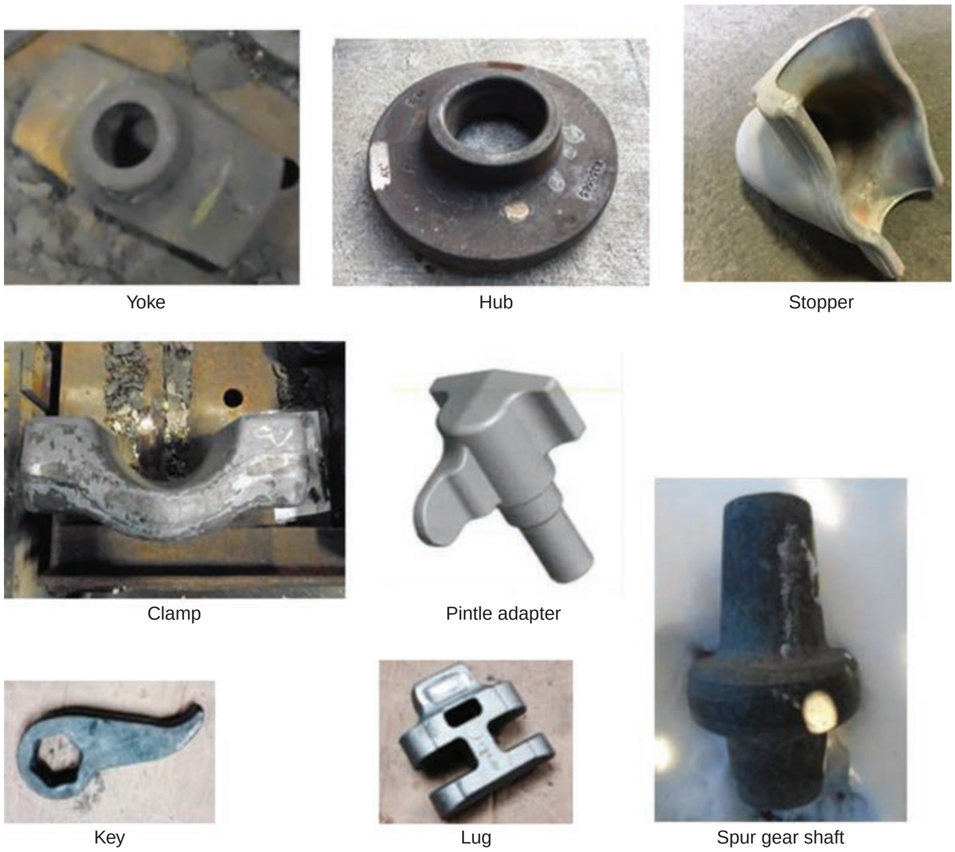

Fig. 26 Examples of forgings hardened using the DFIQ™ process

Table 17 Key mechanical properties for different heat-treating processes applied after forging

Steel	Heat-treatment process	Tensile, psi	Yield, psi	RA, %	Elong., %	Impact, ft·lb	Hardness, RC
4140	Conventional	252,000	220,000	26	10	5	49
	DFIQ	266,000	235,000	40	10	11	49
4340	Conventional	262,000	234,000	39	14	8	51
	DFIQ	272,000	236,000	35	8	9	51
8640	Conventional	221,000	178,000	22	12	6	49
	DFIQ	267,000	229,000	36	9	8	51

Table 18 Pintle adapter mechanical properties

Steel	Heat-treating processes applied	Tensile, psi	Yield, psi	RA, %	Elong., %	Impact, lb·ft
4340	Standard	140,000	125,000	60	23	68
	DFIQ	136,000	112,000	55	23	63
4140	DFIQ	134,000	113,000	54	20	63
Pintle adapter specs:		>130,000	–	–	>19.7	–

were still within the specs. Control of the ultimate hot forging temperature and the initial temperature of the forging as presented to the DFIQ unit are critical to proper grain size formation.

Therefore, when using the DFIQ process, special attention should be paid to controlling the forging temperature to avoid negative effects to the grain size of the steel part. The major findings from the initial DFIQ studies are:

- Forging material grain size plays a significant role in the effectiveness of the DFIQ process. A more precise forging temperature control (both for maximum temperature and uniformity) is needed when using the DFIQ process.
- With a proper material microstructure after forging, application of the DFIQ process improves the mechanical properties of parts, allowing, in many cases, a substitution of a lower alloy and less expensive steel for higher alloy steel.
- Use of the DFIQ process allows the manufacturer to eliminate post-forging heat treatment, resulting in a significant reduction of the heat treatment costs.
- Additional savings from the DFIQ process come from the elimination of shipping costs and lead time between forging and heat-treating shops for reduced work in process inventories. For example, the pintle adapters subjected to the DFIQ process followed by furnace tempering met the customer specifications without being normalized, then annealed, re-austenitized, quenched in oil, and tempered.
- In addition, the DFIQ forgings have very little surface scale, since the parts are not reheated two times after the initial billet heating. In addition, the intensive water quench actually blasts off any forging scale, so shot blast cleaning of the forgings can also be eliminated.
- Since the DFIQ process consistently quenches the part, just as with all IQ processes, it aids in the production of a more predictable near net shape of the part after hardening.

REFERENCES

1. N.I. Kobasko, *Steel Quenching in Liquid Media under Pressure*, Naukova Dumka, 1980, p 206
2. N.I. Kobasko, M.A. Aronov, J.A. Powell, and G.E. Totten, *Intensive Quenching System: Engineering and Design*, ASTM International, 2010, p 234
3. M.A. Grossmann, *Principles of Heat Treatment*, American Society for Metals, 1964, p 303
4. G.E. Totten, C.E. Bates, and N.A. Clinton, *Handbook of Quenchants and Quenching Technology*, ASM International, 1993, p 513
5. H.J. French, *The Quenching of Steels*, American Society for Steel Treating, 1930
6. A.V. Lykov, *Teoriya Teploprovodnosti* [Theory of Heat Conductivity], Vysshaya Shkola, 1967, p 596
7. N.I. Kobasko and H.I. Zhovnir, Analytical Method of Solving Thermal Problems for Steel Quenching, *Visnyk of Academy of Sciences of Ukrainian SSR* (No. 12), 1979, p 41–50
8. N.I. Kobasko, Intensive Steel Quenching Methods, *Theory and Technology of Quenching*, B. Liscic, H.M. Tensi, and W. Luty, Eds., Springer-Verlag, 1992, p 367–389
9. N.I. Kobasko, Intensive Steel Quenching Methods, *Quenching Theory and Technology* (Second Edition), B. Liscic, H.M. Tensi, L.C.F. Canale, and G.E. Totten, Eds., CRC Press, 2010, p 509–567
10. N.I. Kobasko, "Transient Nucleate Boiling as a Law of Nature and a Basis for Designing of IQ Technologies," 7th IASME/

WSEAS International Conference on Heat Transfer, Thermal Engineering and Environment (THE'09), Moscow, 2009, p 67–75
11. N.I. Kobasko, Investigation of batch intensive quenching processes when using hydrodynamic emitters in quench tanks, *EUREKA: Physics and Engineering* (No. 6), 2016, p 29–36
12. M.A. Aronov, N.I. Kobasko, J.A. Powell, and G.F. Totten, Intensive Quenching of Steel Parts, *ASM Handbook Steel Heat Treating Fundamentals and Processes*, Vol 4A, 2013, p 198–212
13. M.A. Mikheev and I.M. Mikheeva, *Osnovy Teploperedachi* [Basics of Heat Transfer], Energy, 1977, p 344
14. H. Martin, Impinging Jets, *Hemisphere Handbook of Heat Exchanger Design*, G. F. Hewitt, Ed., Hemisphere, 1990
15. J. Rath, T. Lübben, M. Hunkel, F. Hoffmann, and H. W. Zoch, Grundlegende Untersuchungen zur Erzeugung von Druckeigenspannungen durch Hochgeschwindigkeits-Abschrecken, *HTM Journal of Heat Treatment and Materials*, Vol 64 (No. 6), 2009, p 338–350
16. J. Rath, T. Luebben, F. Hoffmann, and H. W. Zoch, Generation of compressive residual stresses by high speed water quenching, *International Heat Treatment and Surface Engineering*,Vol 4 (No. 4), 2010, p 156–159
17. H.W. Zoch, R. Schneider, and T. Luebben, Proc. of European Conference on Heat Treatment and 21st IFHTSE Congress, Munich, Germany, 2014, p 566
18. N.I. Kobasko, M.A. Aronov, K. Ichitani, M. Hasegava, and K. Noguchi, High compressive residual stresses in through hardened steel parts as function of Biot number, *Recent Advances in Fluid Mechanics, Heat & Masss Transfer and Biology*, K. Manoj, Jha, et. al, Eds., WSEAS Press, 2012, p 35–40
19. N.I. Kobasko, V.S. Morganyuk, and V.V. Dobrivecher, Control of residual stress formation and steel deformation during rapid heating and cooling, *Handbook of Residual Stress and Deformation of Steel*, G. Totten, M. Howes, and T. Inoue, Eds., ASM International, 2002, p 312–330
20. N.I. Kobask, W.S. Morhuniuk, and B.K. Ushakov, Design of steel-intensive quench processes, *Handbook of Metallurgical Process Design*, G.E. Totten, Kiyoshi Funatani, Lin Xie, Eds., Marcel Dekker, 2004, p 733–764
21. M.A. Aronov, N.I. Kobasko, and J.A. Powell, "Basic Principles and Metallurgy of Intensive Quenching Methods," Proceedings of the 13th IFHTSE Congress, Columbus, Ohio, 2002
22. B.L. Ferguson, A.M. Freborg, and Z. Li, "Residual Stress and Heat Treatment—Process Design for Bending Fatigue Strength Improvement of Carburized Aerospace Gears," European Conference on Heat Treatment, Berlin, 2007
23. M.P. Muhina, N.I. Kobasko, and L.V. Gordejeva, Hardening of Structural Steels in Chloride Quench Media, *Metaloved. Term. Obrab. Met.,* Sept 1989, p 32–36 (in Russian).
24. Ukrainian Patent UA 114174, C2, Alloyed Low Hardenability Steel and Method of its Designing, Filed on Sep. 23, 2013, File number: a 2013 11311, Published on June 25, 2016 in Bulletin No. 12, (Legal day is May 10, 2017)
25. Nikolai Kobasko, *Optimal Hardenability Steel and Method for its Composing*, Lambert Academic Publishing, 2018, p 1
26. Nikolai Kobasko, *Advanced quenching technologies*, Lambert Academic Publishing, 2021, p 119
27. K.Z. Shepelyakovskii, *Strengthening of Machine Components by Induction Surface Hardening*, Mashinostroenie, 1972
28. Boris K. Ouchakov and Konstantin Z. Shepelyakovskii, New Steels and Methods for Induction Hardening of Bearing Rings and Rollers, *Bearing Steels: Into the 21st Century,* ASTM STP 1327, J.J.C. Hoo, Ed., American Society for Testing of Materials, 1998, p 307–320
29. K.Z. Shepelyakovswkii and F.V. Bezmenov, New Induction Hardening Technology, *Advanced Materials & Processes*, October, 1998, p 225–227
30. Russian Patent No. 2158320, Construction Steel of Low Hardenability, Application No. 99125102, Filed on Nov. 29, 1999
31. N.I. Kobasko, Intensive Hardening Method for Metal Components, MPK: C21D 1/63 (2006.01), C21D 1/56 (2006.01), C21D 1/78 (2006.01), C21D 1/18 (2006.01), Ukrainian Patent, UA № 109572, declareted: 07.10.2013; published: 10.09.2015, Bul. 17/2015
32. N.I. Kobasko, Investigation of batch intensive quenching processes when using hydrodynamic emitters in quench tanks, *EUREKA: Physics and Engineering* (No. 6), 2016, p 29–36
33. N.I. Kobasko, Quenching Apparatus and Method for Hardening Steel Parts, U.S. Patent No. 6,364,974 BI, April 2, 2002
34. A. Banka, J. Franklin, B.L. Ferguson, Z. Li, and M. Aronov, "Applying CFD to Characterize Gear Response during Intensive Quenching Process," Proceedings of 24th ASM Heat Treating Conference, Detroit, Michigan, 2007
35. M.L. Bernshtein, Thermomechanical Treatment of Metals and Alloys, *Metallurgiya*, Vol 1, 1968, p 586
36. M.L. Bernshtein, Thermomechanical Treatment of Metals and Alloys, *Metallurgiya*, Vol 2, 1968, p 575
37. I. Tamura, C. Ouchi, T. Tanaka, and H. Sekine, *Thermomechanical Processing of High Strength Low Alloy Steels,* Butterworths, 1988
38. N.I. Kobasko, Thermal and Metallurgical Basics of Design of High-Strength Steels, *Intensive Quenching Systems: Engineering and Design*, N.I. Kobasko, M.A. Aronov, J.A. Powell, and G.E. Totten, Eds., ASTM International, 2010, p 1 – 23
39. M.A. Aronov and J.A. Powell, Forging Process Improvement Using Intensive Quenching Immediately After Forging Operations are Completed, Proceedings of the Forging Industry Association Technical Conference, Columbus, Ohio, 2016